



Article

Soils on Recent Tephra of the Somma–Vesuvius Volcanic Complex, Italy

Antonella Ermice ^{1,*} and Carmine Amalfitano ²

¹ Department of Environmental, Biological, Pharmaceutical Sciences and Technology, University of Campania “Luigi Vanvitelli”, 81100 Caserta, Italy

² Department of Agriculture, University of Naples “Federico II”, 80133 Naples, Italy; carmine.amalfitano@unina.it

* Correspondence: antonella.ermice@unicampania.it

Abstract: The Somma–Vesuvius volcanic complex emitted huge quantities of volcanic materials over a period from before 18,300 years BP to 1944. The activity during the last period, from post-AD 1631 to 1944, primarily produced lava and pyroclastics via effusive and strombolian eruptions. We investigated the pedogenesis on rocks formed from post-AD 1631 to 1944, occurring on the slopes of Mt. Vesuvius up to *Gran Cono Vesuviano* and in the northern valley separating Vesuvius from the older Mt. Somma edifice. Pertinent morphological, physical, chemical, and mineralogical (XRD and FT-IR) soil properties were studied. The results indicated the existence of thin and deep stratified soils on lava, as well as the presence of loose detritic covers formed via pyroclastic emplacement and redistribution. The soils showed minimal profile differentiation, frequently with layering recording the episodic addition of sediments. We found that the dominant coarse size of primary mineral particles was preserved, and there was a low level of clay production. The main mineralogical assemblage present in sands also persisted in clays, indicating the physical breaking of the parent material. Chemical weathering produced mineral modifications towards the active forms of Al and Fe and was also attested in selected soils by glass alteration, allophane production, and the presence of analcime in clay as a secondary product from leucite. The differences in glass alteration and analcime production found in the selected soils on lava were related to soil particle size and soil thickness. Concerning the youngest soil present on *Gran Cono Vesuviano*, other factors, such as the substratum’s age and site elevation, appeared to be implicated.

Keywords: recent volcanic soils; soil mineral weathering; glass alteration; XRD soil analysis; FT-IR soil analysis



Citation: Ermice, A.; Amalfitano, C. Soils on Recent Tephra of the Somma–Vesuvius Volcanic Complex, Italy. *Soil Syst.* **2024**, *8*, 50. <https://doi.org/10.3390/soilsystems8020050>

Academic Editor: Antonio Martínez Cortizas

Received: 7 November 2023

Revised: 9 January 2024

Accepted: 30 January 2024

Published: 30 April 2024



Copyright: © 2024 by the authors. Licensee MDPI, Basel, Switzerland. This article is an open access article distributed under the terms and conditions of the Creative Commons Attribution (CC BY) license (<https://creativecommons.org/licenses/by/4.0/>).

1. Introduction

Volcanoes are a source of instantaneous production of mineral matter, which allows the rapid regeneration of rock stocks on Earth, offering new opportunities for pedogenetic activity. In a volcanic environment, substrata are involved in pedogenesis through the volumes and kinds of volcanic deposits, the dispersion and selection of fall materials during transportation, tephra layering [1,2], and weathering processes which occur primarily at the expense of glass components [1,3]. The volcanic substrata supply also affects the composition of vegetation and microbes depending on the amount of disturbance [4]. Gas emissions and acidic rain also play important roles in tephra alteration [1,2,5,6] in sites near the emission center [7,8]. Most importantly, volcanic substrata are entities with particularly limited lives due to the easy alterability of most components of volcanic rocks [9,10], usually tending to undergo rapid modifications toward soil formation. Therefore, young volcanic pedogenetic environments are suitable for exploring the effects of active components in transformation processes over short time spans and to depict their possible impact on soil formation. The interest in the study of the first stages of weathering toward soil formation in

volcanic environments is testified by the numerous geochemical, mineralogical, ecological, and pedological studies conducted in various parts of the world. These are exemplified in [11–22], among others.

Just as in other parts of the world, the presence of volcanoes and their effects on the physical environment are experienced across the European continent and its islands. Here, soils with properties dominated by tephra weathering (andic soil properties)—categorized as Andosols according to the World Reference Base for Resources (WRB) classification system, or as Andisols or Andepts according to the USA Soil Taxonomy (ST) classification system—are recognized. Nevertheless, other soils are also found due to the variety of climates, geomorphologies, vegetation, land uses, and tephra ages and compositions. These include the following: Cambisols (WRB) or Inceptisols (ST), which are widespread; Podzols (WRB) or Spodosols (ST), found in France and Italy; Umbrisols (WRB), found in Hungary and the Carpathian Basin, where Phaeozems and Luvisols (WRB) are also present, the former also found on Madeira Island and the latter in Germany, Italy, and the Canary Islands; Vertisols (WRB and ST), present on Madeira Island and the Canary Islands, with Aridisols (ST) also recorded; Calcisols (WRB), found in Spain, where soils with andic soil properties are not recognized; Mollisols (ST), discovered in Italy. Additionally, weakly developed soils such as Vitrisols (WRB) in Iceland, Regosols (WRB), Leptosols (WRB), or Entisols (ST) in Greece, Italy, Spain, the Canary Islands, and Madeira Islands are also found, as shown in [23] and in references therein.

In particular, extensive areas affected in various ways by tephra and related volcanogenic soil covers are found in southern Italy, as shown in [15,17,24–31], among other articles. Here, Vesuvius provides the opportunity to study the first stages of pedogenesis because of its eruptive activity, dating from before 18,300 years B.P., which endured until the 1944 eruption. This event closed the last Vesuvian eruptive period (from post-1631 to 1944), which experienced numerous eruptions in rapid succession [32,33]. The volcanic district in question is also a robust candidate for the study of young soils due to the non-extreme climatic conditions, excluding accelerations or decelerations of weathering processes, and the almost basaltic composition of the recent substrata [34], which confers weak resistance to alteration [1]. The physical environment in question also exhibits characteristics which are also found in other young volcanic areas. These are: (i) the presence of lavas and pyroclastic rocks, with the latter having variable thicknesses [35] depending on the event entity; (ii) variation in the local microtopography; (iii) reworking processes, which may compromise the temporal uniformity of a single pyroclastic deposit, an effect which is also produced by the inclination of the edifice walls; (iv) the cone-shaped morphology of Vesuvius [36], implicating variations in altitude, orientation, and vegetation, with the latter also being affected by reforestation interventions [37]; (v) gas emissions, which, currently limited to the inner ring and floor of the crater, occurred on the outer flanks of Vesuvius during the inter-eruptive periods and persisted for several months after the 1944 event [38,39]; (vi) acid rainfall, with a pH from about 2.5 to 3 [40,41], coinciding with the most recent volcanic episodes; and (vii) marine aerosol, influencing the composition of rainwater due to the geographical position of Somma–Vesuvius [42]. These concerns depict a variety of conditions that are potentially implicated in soil formation and which can contribute to differentiating pedogenetic pathways and outcomes.

The investigations conducted on Vesuvian soils mainly consider those formed from the products of events older than the last activity period, accounting for the distribution and variety of their stratigraphic, chemical, and mineralogical characteristics, as shown in [26–29,39,43–47], among others. The less extensive literature available on soils formed from products deposited during the recent Vesuvian activity focuses mainly on the young age and frequent renewal of the volcanic substrata [24,25,28,48–50]. There is less emphasis on the high phenomenic diversity of the recent Vesuvian environment. This study explores the early-stage pedogenesis on recent Vesuvian tephra, from post-AD 1631 to 1944, with the following aims: (i) to better understand the soil's genesis, morphology, and selected properties and (ii) to investigate the major factors and processes active in such a young

geological environment. The soil locations comprised the slopes of Vesuvius up to the volcano's *Gran Cono Vesuviano* and the caldera floor of Mt. Somma, where the recent Vesuvian tephra is primarily concentrated. The study area, forming part of the Vesuvius National Park, represents a physical context with intrinsic environmental value due to its major landscape-related and geological significance.

2. Environmental Setting

The study was conducted on the Somma–Vesuvius volcanic complex, a composite volcanic system located about 15 Km ESE of Naples (Figure 1). Somma–Vesuvius consists of the older Mt. Somma (1132 m a.s.l.) caldera, of which only the northern wall is preserved, and of the recent cone of Vesuvius (*Gran Cono Vesuviano*) (1281 m a.s.l.), which formed in the Mt. Somma caldera [35] (Figure 1). Somma–Vesuvius activity refers to four periods [34]: pre 18,300 B.P. [33], before the formation of the Mt. Somma caldera; from 18,300 B.P. to AD 79, corresponding to the start of the formation of the Mt. Somma caldera; from AD 79 to 1631, starting with Pompeii's Plinian eruption and ending with the small-scale 1631 Plinian eruption; and from post-1631 to 1944 period. The first period was characterized by a primarily effusive eruptive style. The second and third periods were those dominated by major explosive events, and the last period experienced semipersistent activity, including totally effusive, strombolian, violent strombolian, and a few sub-Plinian eruptions. During the last period, there were 99 eruptions in total, which were separated by short, quiet periods that never exceeded seven years [51]. Pumices are the magmatic products typical of explosive eruptions, while effusive eruptions mainly produce lava flows with ashes, lapilli, and blocks [34]. The current architecture of the volcanic system is a result of the progressive collapse, caused by the Plinian eruptions from 18,300 years B.P. to AD 79, of the SSW wall of the Mt. Somma caldera [52] in which Vesuvius formed. A surface strip (Valle del Gigante) within the Mt. Somma caldera separates the area between the remaining edifice of Mt. Somma and the northern wall of Vesuvius. The lava flows of the last period, emitted from the Vesuvian crater and lateral vents [35,53], could not flow down the slopes of the Mt. Somma edifice due to the barrier constituted by the remaining wall of the old caldera. At the same time, they spread across extensive portions of the Vesuvian slopes and the floor of the caldera separating the two volcanic structures. The result was the formation of interconnected tongues typically depicting these volcanic sectors (Figure 1A). By contrast, coeval air-fall products were distributed across all volcanic sectors of both Mt. Somma and Mt. Vesuvius. On Mt. Somma, these products stratified on those of previous volcanic activity, while on Mt. Vesuvius they covered the recent lava flows [35]. Processes of remobilization of loose pyroclastics, triggered by rainfall, also affected the surfaces [35,54], in particular on the northern and eastern volcanic sectors, displaying major intensity on the flanks of Mt. Somma and *Gran Cono Vesuviano* [55]. Morphologically, the northern flank of Mt. Somma and the slopes of *Gran Cono Vesuviano* exhibit the highest steepness, contrasting with the more gently degrading seaward-facing slopes of Vesuvius [36].

The products from the last period of the volcanic activity vary from leucititic tephrites to leucititic phonolites [34]. They have the compositions of the highly SiO₂-undersaturated Vesuvian rocks. The latter are the Vesuvian rocks with the lowest SiO₂ contents (47.0% to 51.0%). They also exhibit higher Al₂O₃ contents, with few exceptions exceeding 17%, as well as the highest levels of CaO. Additionally, there are irregular increases in Na₂O and K₂O [34,56]. The most common minerals are clinopyroxenes, leucite, feldspars, which are mainly plagioclases, minerals of the olivine group, biotite, Fe-Ti oxides, and volcanic glass which contributes to the mineralogical composition of the recent Vesuvian tephra by about 50% [34,35,57].

The area has a Mediterranean climate, with an average annual temperature of 15 °C and an average annual rainfall of 950 mm. On the slopes of Vesuvius, from approximately 100 m up to 700–800 m a.s.l., the vegetation consists of *Quercus ilex*, which is more often found mixed with *Pinus pinea* and *Pinus halepensis*, two species used in the area for forestation, and with *Cytisus scoparius*, *Genista aetnensis*, and *Robinia pseudoacacia*. At higher

elevations, there are large areas of vegetation consisting of shrubs (*Rumex scutatus*, *Artemisia variabilis*, *Scrophularia canina*, *Silene vulgaris*, *Cytisus scoparius*, frequent *Spartium junceum*, *Genista aetnensis*, and *Robinia Pseudoacacia*). These extend up to approximately 1000 m a.s.l. and are also found on the Mt. Somma caldera floor, where also coniferous and deciduous species grow. Shrubs also occur very sparsely on the summit of the *Gran Cono Vesuviano* and in smaller patches at medium elevations. Small areas with *Castanea sativa* are found at various elevations and exposures [37,58]. Extensive areas of the lower Vesuvian strip, up to about 100–350 m a.s.l., are either urbanized or used for agricultural purposes.

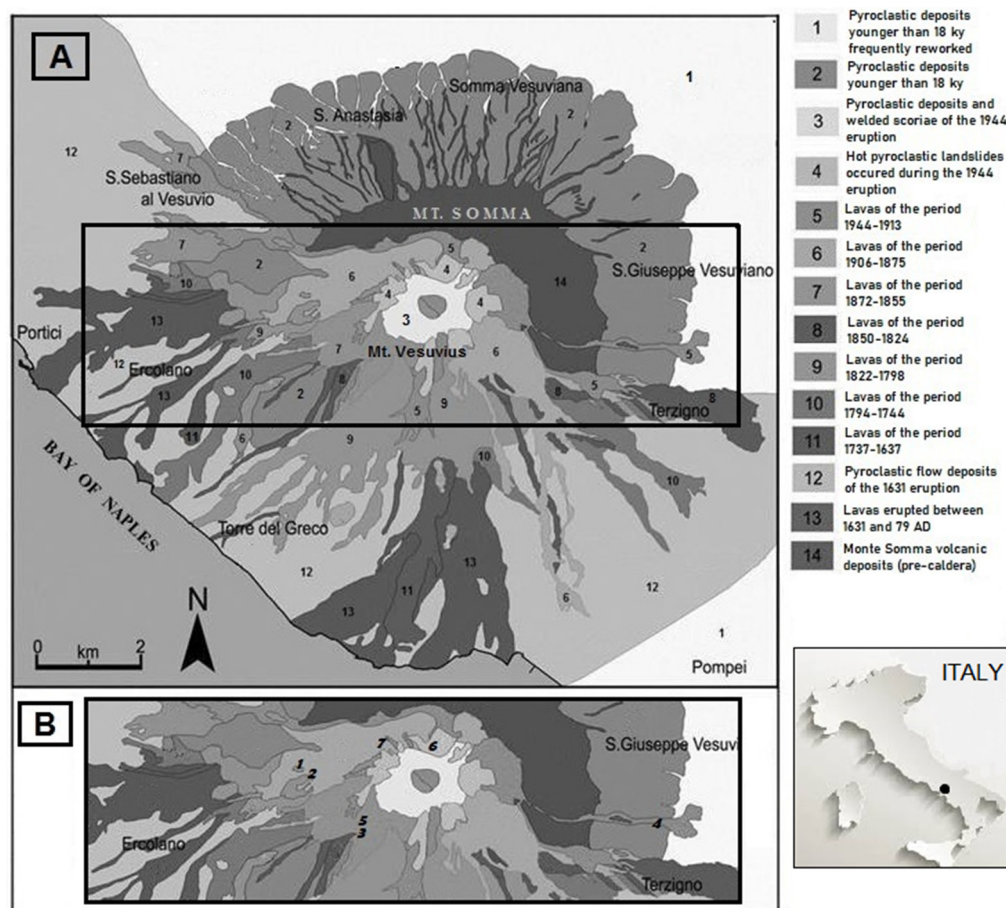


Figure 1. (A) A simplified geological map of the Somma–Vesuvius volcanic complex (modified from Orsi et al. [59]). (B) The location of the studied soils.

3. Materials and Methods

The soils studied were located on the slopes of Vesuvius up to *Gran Cono Vesuviano* and on the northern valley separating Vesuvius from the older Mt. Somma volcanic edifice. These areas, both natural areas and those characterized by human disturbance, assured the presence of recent Vesuvian products [35]. Within the study area, seven soils (Figure 1B) were selected among sites with different elevation, exposure, and vegetation. The sites were at elevations ranging from 186 to 1050 m a.s.l. along southwestern, southern, eastern, and northern orientations, with vegetation varying from forests to shrubs. Soils 1 to 5 and Soil 7 were present on lava flows outcropping at different depths. Soil 6 was selected as being representative of a fresh cover of fall products that were deposited from the last 1944 Vesuvius eruption on the *Gran Cono Vesuviano*. Two soil profiles (Soils 1 and 3) were reviewed from a previous survey [25]. The pertinent characteristics of the selected soil locations are listed in Table 1. For sites 1–5 and 7, the age reported is that of the respective outcropping lavas. In fact, the overlying fall deposits can be derived from the same event

that generated lava and/or from other recent events as a result of sediment redistribution along the slopes of the volcanic edifice. In this scenario, complex tephrostratigraphic correlations must be combined with the analysis of historical records in order to confidently reconstruct the temporal relations between lavas and overlying pyroclastics, as well as to discern the relations between pyroclastic layers, as outlined in [35] and references therein. This circumstance prevents the investigation of direct relations between soil properties and age for most soil profiles. In this study, the attribution of a reliable age of fall deposits was only possible for Soil 6 on *Gran Cono Vesuviano*, a site uniformly characterized by the accumulation of pyroclastics from the last 1944 eruption [60,61].

Table 1. Pertinent characteristics of the selected soil locations.

| Site/Soil | Outcropping Substrata | Elevation m a.s.l. | Exposure | Soil Use |
|-----------|---------------------------|-----------------------|----------|--------------------------------------|
| 1 | 1858 lava flow | 530 | SW | Pine forest with <i>Quercus ilex</i> |
| 2 | 1858 lava flow | 670 | SW | Oak with pine plantation |
| 3 | Pyroclastics on 1872 lava | 650 | S | Pine forest with <i>Quercus ilex</i> |
| 4 | Pyroclastics on 1929 lava | 186 | E | Oak plantation |
| 5 | 1872 lava flow | 670 | S | Pine forest with <i>Quercus ilex</i> |
| 6 | 1944 pyroclastics | 1050 | N | Sparse spots of shrub vegetation |
| 7 | 1891–94 lava flow | 930 | N | Sparse shrub vegetation |

Except for Soil 6, the soils were excavated to the depth of the top of the lithic contact constituted by lava layers. In the field, the following morphological features were described [62]: horizon or layer depth, color, moisture, texture, rock fragments, structure, consistency, and horizon boundaries. Bulk samples were collected from each horizon or layer and air-dried for the following analyses: particle-size distribution [63], where the 2.0–0.2 mm soil mineral particles were assessed by wet sieving, and the 0.2–0.02 mm, 0.02–0.002 mm and <0.002 mm particles by the sodium hexametaphosphate dispersion method; available water content (AWC) was determined by calculating the difference in water retention at 33 kPa and 1500 kPa using the literature values [64]; organic C content, was determined using the Walkley–Black oxidation method [65]; soil reaction (pH), was measured in water suspensions (1:2.5 soil/solution), and CaCO₃ content was assessed by treatment with excess HCl and volumetric determination of CO₂ [66]. Regarding the development of amorphous mineral components, which is considered in the study of volcanogenic pedogenesis [3,67], oxalate extractable Al (Alox) and Fe (Feox) [68], as well as P retention [69], were determined.

In order to determine the chemical properties useful to ascertain mineral modifications, three soils were selected: Soils 1 and 3 because, among the soils analyzed, they had similar location features but differed in texture and thickness, and Soil 6 because it was formed from the most recent pyroclastics (AD 1944). In particular, pyrophosphate extractable Al (Alp) [69] and oxalate extractable Si (Siox) [68] were determined in order to calculate the Al/Si ratio (obtained as Alox-Alp/Siox) in the noncrystalline materials [70]. Following the method of Mizota and Reeuwijk [70], the allophane content was estimated in the specimens where the Al/Si ratio was ≥ 1 . Except for Soils 6 and 7, for which the classification procedure was not applied, soils were classified according to Soil Survey Staff [67].

Powder X-ray diffraction (XRD) and infrared spectroscopy (FT-IR) analyses were performed on the 2–0.2 mm (sand) and <0.002 mm (clay) fractions. XRD analysis was conducted using a Rigaku Geigerflex D/MAX B diffractometer, using an Fe-filtered CoK α radiation (40 kV and 30 mA, 2° min⁻¹ scanning speed, three runs accumulated). XRD spectra were interpreted in accordance with the Joint Committee on Powder Diffraction Standards [71]. In order to verify the possible production of leucite artifacts caused by contact with Na⁺ from sodium hexametaphosphate [72], XRD analysis of clay obtained from some samples via sedimentation in deionized water was performed. XRD analysis was

also conducted on crushed >2 mm fractions (rock fragments). The spectra were obtained by the KBr disk method (1% *w/w*) using a Perkin Elmer 1720X FT-IR spectrometer.

In order to compare the relative variation in leucite and analcime in sands and clays, we calculated the intensity ratio of the X-ray reflection of analcime at 0.560 nm and that of leucite at 0.538 nm (analcime/leucite ratio) for Soil 1, selected soil horizons from Soil 3, and Soil 6. FT-IR analysis was performed on the powdered sands, on clays, and on analcime-stripped clays from the Bw soil horizon of Soil 1, obtained by 0.5 M HCl treatment for 4 h at room temperature [73]. Simple linear regression was used to analyze the relationships among some of the investigated soil properties, and those between the latter and site elevation. In the last case, weighted means of the soil properties considered were used.

4. Results

4.1. Morphological Features

The morphological characteristics of the soil profiles are shown in Table 2. Except for Soil 6, the soil morphology was characterized by lithic contact, which, at various depths, consisted of lava deposits (R and R/C horizons). The latter were overlaid by soil covers with thicknesses ranging from 30–70 cm (Soils 1, 2, 5, and 7) to 100–160 cm (Soils 3 and 4). The surface A soil horizons were frequently under organic layers and, except when Bw soil horizons were found, directly overlaid on one or more C soil horizons. The latter frequently ranged from gravelly to extremely gravelly [62]. They mainly consisted of lithic fragments, loose crystals, and scoria, which, in the layers directly lying on lava, were also mixed with lava blocks. In Soils 3, 4, and 7, the irregular variation in rock fragment content along the soil depth and the change in soil color suggested discontinuities in the soil horizon sequence. Buried soil horizons (2ABb) were found in the two deeper soil profiles (Soils 3 and 4). Soil 6 mainly consisted of coarse and loose pyroclastics, resulting in a very poorly organized soil profile, where only a very weak aggregation and finer rock fragments distinguished the upper layer from the underlying portion. Most of the soil horizons had coarse textures. A finer texture was observed in Soil 1. Very weak and weak structure, or the absence of structure, and very friable, friable, or loose consistency characterized most of the soil horizons. The horizon boundaries, when not clear, were abrupt, often coinciding with the lithological discontinuities.

Table 2. Morphological characteristics of the selected recent Somma–Vesuvius soils.

| Soil | Horizon | Depth cm | Dry Color | >2 mm Fragments ^b and Texture ^c | Structure ^d | Consistency ^e | Boundary ^f |
|----------------|------------------|-------------|-----------------------------------|--|------------------------|--------------------------|-----------------------|
| 1 ^a | A | 0–5 | 10YR 3/2 | f/m sl | 3f/msbk | fr | cw |
| | Bw | 5–30 | 10YR 3/4 10YR 4/4 (moist) | f/m/c sl | 3msbk | mfr | cw |
| 2 ^a | (2)R/C | 30+ | - | - | - | - | - |
| | A | 0–30 | 10YR 3/4 10YR 4/4 (moist) | f/m/cg ls | 2f/m sbk | vfr | aw |
| | Bw | 30–68 | 5YR 3/3 | mvg/co sl | 3msbk | l | cw |
| 3 ^a | (2)R/C | 68+ | - | - | - | - | - |
| | A | 0–15 | 5YR 3/2 5YR 3/1 | f/m/cvg ls | 2f/m sbk | fr | cs |
| | C | 15–20 | 5YR 3/1 5YR 2.5/1 5YR 2.5/2 | c/feg s | 0sg | l | as |
| | 2ABb | 20–31 | 5YR 3/3 | fg ls | 2m/c sbk | fr | cw |
| | 2C1 | 31–45 | 5YR 2.5/1 | f/mg s | 0sg | l | aw |
| | 3C2 | 45–60 | 10YR 3/2 | f/mvg s | 0sg/1f sbk | l/vfr | as |
| | 4C3 ^g | 60–77 | 10YR 3/1 | f ls | 0ma | fr | - |

Table 2. Cont.

| Soil | Horizon | Depth | Dry Color | >2 mm Fragments and Texture ^b | Structure ^d | Consistency ^e | Boundary ^f |
|----------------|------------------|---------|-------------|--|------------------------|--------------------------|-----------------------|
| | | | 7.5YR 3/1 | | | | |
| | | | 7.5YR 3/2 | | | | |
| | 5C4 | 77–85 | 5YR 4/2 | s | 0ma | mfr | aw |
| | 6C5 | 85–92 | 10YR 4/1 | m/ceg ls | 0sg | l | as |
| | 7C6 | 92–94 | 5YR 3/3 | ls | 0ma | vfr | aw |
| | 8C7 | 94–102 | 5YR 3/1 | m/ceg/co s | 0sg | - | - |
| | (9)R | 102+ | - | - | - | - | - |
| 4 ^a | A | 0–7 | 2.5YR 2.5/2 | m/fvg ls | 0sg | l/vfr | cw |
| | C | 7–65 | 7.5YR 2.5/1 | m/cvg s | 0sg | l/vfr | cw |
| | 2ABb | 65–70 | 10YR 3/2.5 | f/m/cg ls | 0/1f sbk | vfr | cw |
| | 2C1 | 70–85 | 7.5YR 3/2 | f/mvg s | 1f sbk/0sg | vfr/l | cw |
| | 3C2 | 85–90 | 10R 3/2 | f/m ls | 1f/m sbk | fr | cw |
| | 4C3 | 90–95 | 2.5YR 2.5/2 | f/mvg s | 0sg | l/vfr | cw |
| | 5C4 | 95–97 | 10YR 3/2 | c | 1f/m sbk | fr | as |
| | 6C5 | 97–103 | 10R 2.5/2 | f ls | 1m sbk | fr | as |
| | 7C6 ^g | 103–108 | 5YR 3/1 | - | 1m sbk/0sg | mfr/l | b |
| | 8C7 | 108–150 | 5YR 3/1 | f/m/ceg s | 0/1f sbk | l/fr | as |
| | | | 5YR 3/3 | | | | |
| | 9C8 | 150–160 | 10YR 3/2 | - | 1f/msbk | mfr | as |
| | | | 10YR 3/1 | | | | |
| | (10)R | 160+ | - | - | - | - | - |
| 5 ^a | A | 0–3 | 10YR 3/4 | mg ls | 1f/m gr | vfr | aw |
| | C1 | 3–15 | - | m/ceg s | 1f sbk/0sg | vfr/l | cw |
| | C2 | 15–60 | 10YR 4/2 | co/ceg s | 0sg | l | cw |
| | (2)R | 60+ | - | - | - | - | - |
| 6 | CA | 0–20 | 7.5YR 3/2 | f/m/ceg s | 0sg/1gr | l | cs |
| | C | 20–65 | 7.5YR 3/2 | m/ceg s | 0sg | l | - |
| 7 | A | 0–2 | 5YR 3/2 | f/m/cg s | 0sg | l/vfr | cs |
| | C1 | 2–6 | 7.5YR 3/2 | m/cvg s | 0sg | l | as |
| | 2C2 | 6–20 | 10YR 2/1 | cvg s | 0sg | l | cw |
| | (3)R | 20+ | - | - | - | - | - |

^a Soil with organic Oi and Oe horizons, with thickness from 2 to 4 cm and 1 to 3 cm, respectively. ^b co = cobbly; g = gravelly; e = extremely; v = very; f = fine; m = medium; c = coarse. ^c ls = loamy sand; s = sand; sl = sandy loam. ^d Grade: 0 = structureless; 1 = very weak; 2 = weak; 3 = moderate. Size: f = fine; m = medium; c = coarse. Kind: gr = granular; abk = angular blocky; sbk = subangular blocky; sg = single grain; ma = massive. ^e l = loose; vfr = very friable; fr = friable; mfr = moderately friable. ^f Distinctness: a = abrupt; c = clear. Topography: s = smooth; w = wavy; b = broken. ^g Horizon with pockets of contrasting materials. The slashes indicate that, on the same horizon, there are different sizes and kinds of coarse fragments, as well as different structures and consistencies. The number prefix in parenthesis indicates the possible discontinuity of the R layers with respect to the overlying horizons.

4.2. Physical and Chemical Properties and Soil Classification

The results of the particle-size analyses of the soil profiles are shown in Figure 2. The soils had textures from sand to sandy loam, with total sand ranging from 72.8% to 100%, silt from 0% to 17.5%, and clay from 0% to 10.4%. Soil 1 exhibited the lowest total sand concentration, as found in the field. The estimated AWC values were 5.8% for the sandy samples and 7% for the loamy sandy samples, reaching 11% in the sandy loamy samples.

The results of chemical analyses are shown in Figures 3 and 4 and Table 3. The values of pH(H₂O) (Figure 3) were from slightly acidic to moderately alkaline. The latter was only measured in Soil 6. Organic C contents were very low or low, varying from traces up to 25.5 g kg⁻¹ (Figure 3). The highest organic C values were measured in the upper A soil horizons of each soil profile and in the buried 2ABb horizon of Soils 3 and 4. Here, the organic C contents were 4.0 and 13.3 g kg⁻¹, respectively, which are values comparable to those of the respective upper A horizons (4.3 and 14.5 g kg⁻¹). CaCO₃ was always absent. With respect to the evaluation of amorphous mineral components, the values of Alo_x ranged from 0.53% to 2.6%, and those of Fe_{ox} spanned from 0.23% to 2.3% (Figure 4).

Al/Si ratios, obtained using data of Siox, Alox, and Alp, resulted in 1.0–1.1 for Soil 1, from 1.0 to 1.6 for the selected soil horizons of Soil 3, and 0.6–0.7 for Soil 6 (Table 3). As a consequence, Soil 6 was excluded from the estimation of allophane [70], which, by contrast, amounted to 4.4–4.5% and 2.6–3.8% in Soils 1 and 3, respectively (Table 3).

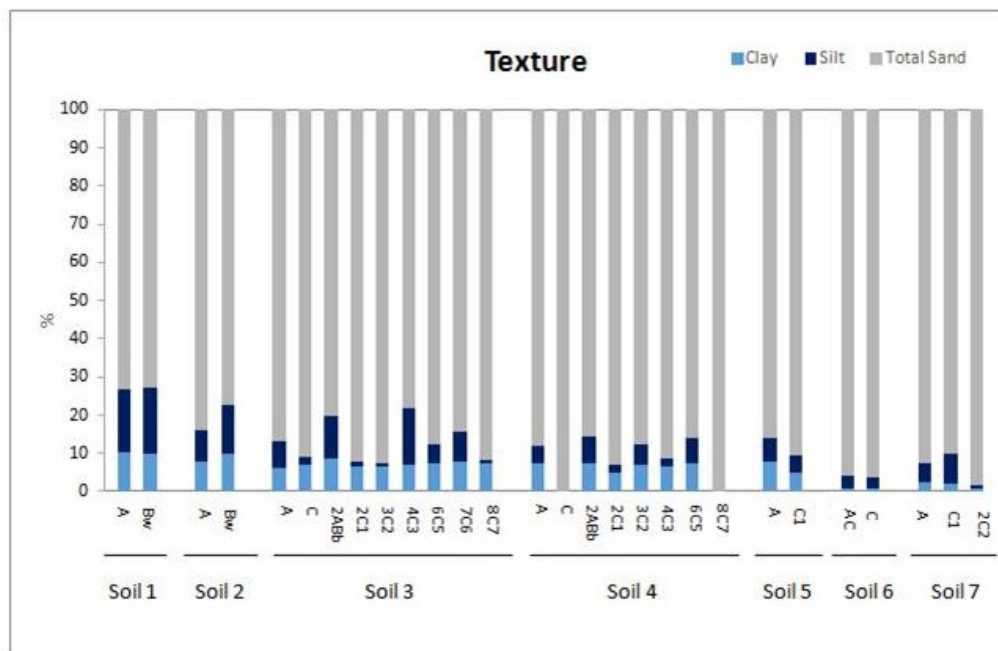


Figure 2. Clay, silt, and sand distribution in the analyzed soil horizons.

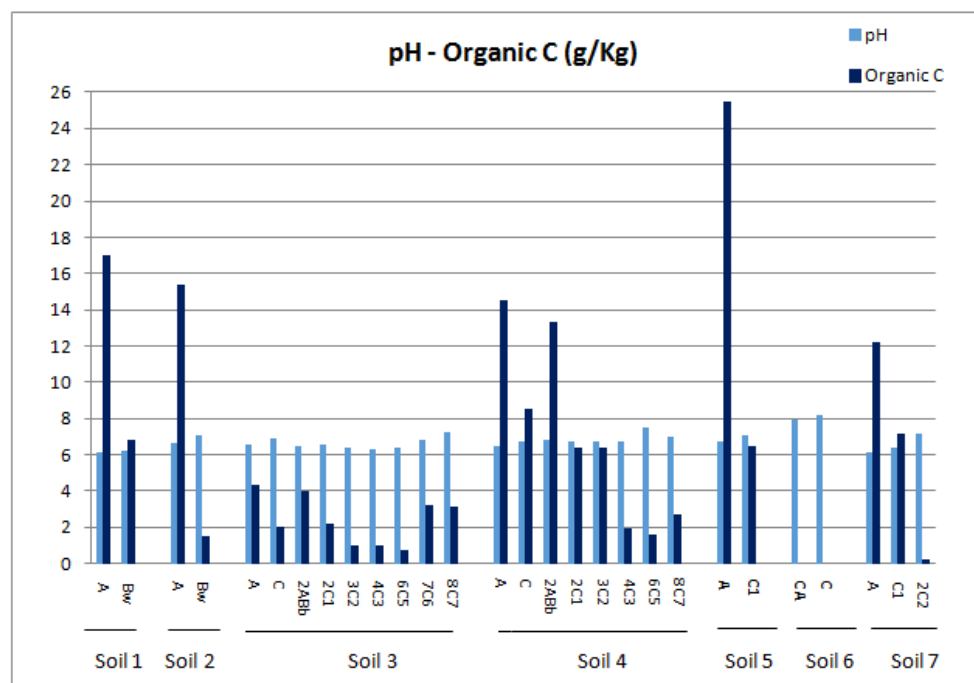


Figure 3. pH and organic C values of the analyzed soil horizons.

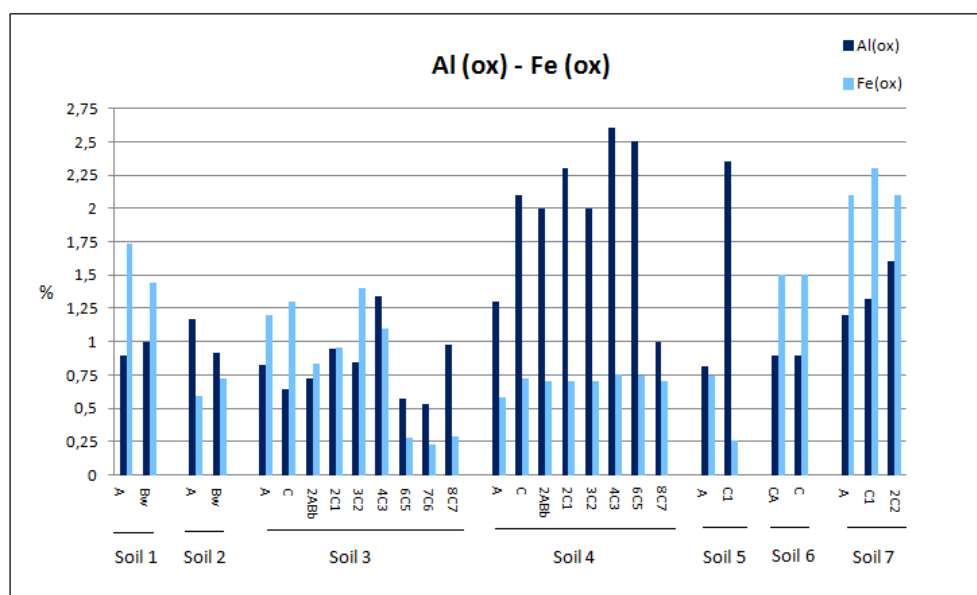


Figure 4. Oxalate extractable Al and Fe values of the analyzed soil horizons.

Table 3. Analyses of noncrystalline components in pertinent horizons of the selected soils.

| Soil | Horizons | Depth cm | Alox | Siox | Alp % | (Alox – Alp)/Siox | Allophane ^a |
|------|----------|-------------|------|------|----------|-------------------|------------------------|
| | | | | | | | % |
| 1 | A | 0–5 | 0.90 | 0.8 | 0.1 | 1.0 | 4.4 |
| | Bw | 5–30 | 1.00 | 0.8 | 0.1 | 1.1 | 4.5 |
| 3 | A | 0–15 | 0.82 | 0.6 | 0.08 | 1.2 | 3.5 |
| | C | 15–20 | 0.64 | 0.6 | 0.04 | 1.0 | 3.3 |
| | 2ABb | 20–31 | 0.72 | 0.4 | 0.09 | 1.6 | 2.6 |
| | 2C1 | 31–45 | 0.95 | 0.6 | 0.06 | 1.5 | 3.8 |
| | 3C2 | 45–60 | 0.84 | 0.6 | 0.06 | 1.3 | 3.6 |
| 6 | CA | 0–20 | 0.90 | 1.3 | 0.02 | 0.7 | - |
| | C | 20–65 | 0.90 | 1.4 | 0.02 | 0.6 | - |

^a: Calculated using $(Alox - Alp)/Siox$, as reported in Mizota and van Rensburg [70].

Concerning soil classification, no andic soil properties were recognized due to the low (<25%) measured P retention values, varying from 0% to 17.7%. Among the other selectable diagnostic horizons, only a weakly expressed cambic horizon was displayed by the Bw horizons of Soils 1 and 2. Moreover, due to the low content of organic C, which suggested that the bulk density values of the fine earth fraction were higher than 1 g/cm^3 [74], and the high volume of the volcanic rock fragments in the pertinent horizon control sections, the soil profiles had vitrandic characteristics, except for the finer and shallower Soil 1. Therefore, Soil 1 was classified as Lithic Haploxerept, Soil 2 as Vitrandic Haploxerept, and Soils 3, 4, and 5 as Vitrandic Xerorthents.

4.3. Mineralogical Features: XRD and FTIR Analyses

The XRD patterns of the sand fractions (2–0.2 mm) extracted from the three selected Soils, 1, 3, and 6, were qualitatively similar and only differed slightly in terms of their relative peak intensities. Pronounced feldspar peaks, including plagioclases (0.327, 0.321, and 0.318 nm, among others), were present, in addition to the peaks of pyroxenes (0.299 and 0.295 nm) and olivines (0.256 and 0.251 nm). Biotite (1.0 nm) was evident in some soil horizons. Leucite was recorded at 0.554, 0.538, 0.343, 0.290, 0.292, 0.284, and 0.280 nm and also contributed to the 0.327 nm signal. Although analcime could contribute to peaks at 0.343, 0.292, and 0.280 nm, in the sand samples the absence or weak intensity of its typical peaks at 0.560 and 0.485 nm suggested that this mineral made a negligible contribution

to the sand composition. Figure 5 shows the XRD pattern of the soil horizons of Soil 1 (see also Supplementary Materials, Figures S1–S4). The above mineral assemblage also characterized the XRDs of the rock fragments (>2 mm) (see Supplementary Materials), which were very similar to those of each respective sand. Despite XRD patterns evidencing a general similarity in mineral composition between fine and coarse fractions, the former differed from the latter in the appearance of analcime peaks at 0.560 and 0.485 nm and in the higher peaks of both leucite and analcime at 0.343 and 0.292 nm. The different contribution made by analcime was corroborated by the analcime/leucite ratio (Figure 6), which was higher in clays than in sands. The participation of analcime in clay fractions was also proved via FT-IR analysis, displaying absorption bands at about 766 and 726 cm^{-1} . These were attributable to analcime [75] and disappeared after treatment with 0.5 M HCl [73] (Figure 7).

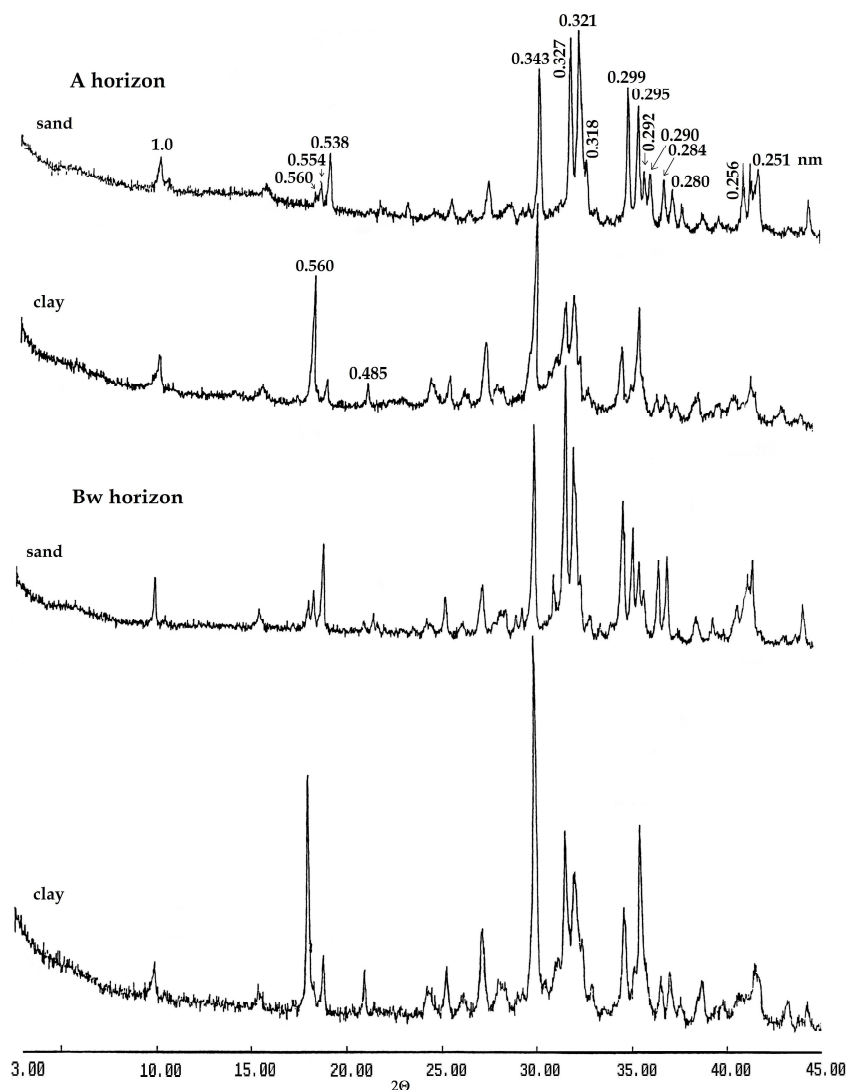


Figure 5. XRD of sand and clay fractions from horizons of Soil 1.

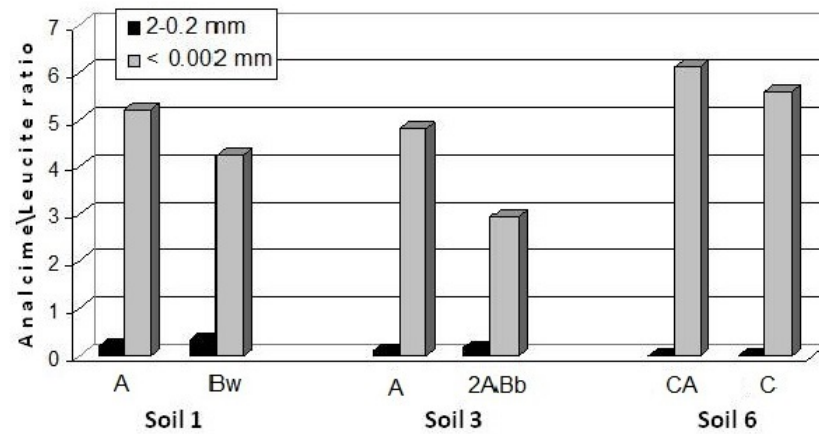


Figure 6. Analcime-to-leucite ratio, calculated as the intensity of the reflections at 0.560 nm for analcime and 0.538 nm for leucite.

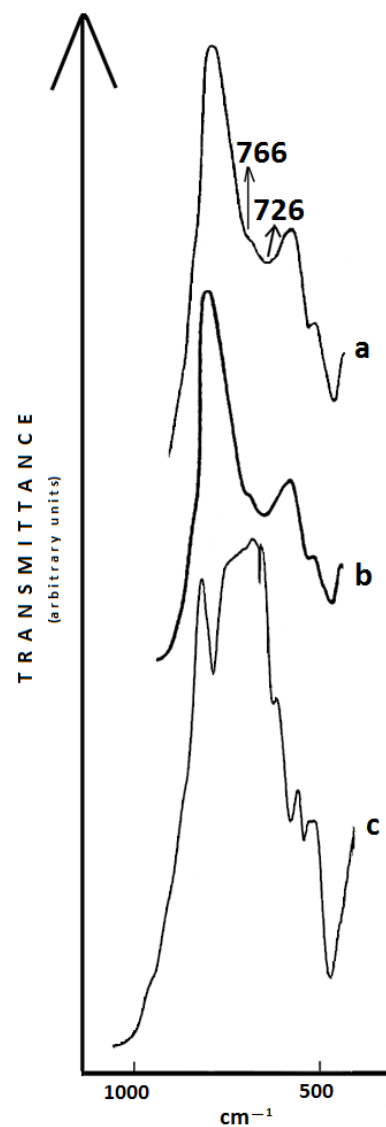


Figure 7. FTIR spectra of clay fractions from A and Bw soil horizons of Soil 1. a: A horizon. b: Bw horizon. c: Clay fraction from analcime stripped Bw horizon.

5. Discussion

5.1. Morphological Features

Three dominant soil morphologies were recognized in the area. These included thin and deep pyroclastic soil profiles (Soils 1, 2, 5, and 7, and Soils 3 and 4, respectively), found on variously fragmented lava tongues at different depths, and a loose detritic soil cover (Soil 6) characteristic of the steep slopes of the Vesuvian summit. In the soils on lava, the soil thickness appeared to be determined by the local accumulation of both air-fall and reworked deposits on microrelief and microdepressions formed by the lava flows.

The diffuse presence of high volumes of pristine coarse rock fragments in the soil horizons could, reasonably, be a consequence of the short distance of the young substrata from the source [76]. Due to the youthfulness of the pedogenetic environment, the soils retained the marks of sedimentogenic activity. In particular, in Soils 3, 4, 5, and 7, the multiple uninterrupted C soil horizons, typically found in young environments with the frequent addition of volcanic materials [1,14,18,77–79], were signs of close sediment gains through fall and/or erosion. The latter process was frequently found to occur on the Vesuvian surfaces [35,54]. The marks of the process in question were recorded in Soils 3 and 4, which contained pockets of contrasting materials within the 4C3 and 7C6 soil horizons, respectively. The occurrence of buried soil horizons in Soils 3 and 4 could be associated with circumstances that, retarding surface burial, favored the start of pedogenetic processes [80].

5.2. Physical Properties: Particle-Size Distribution and AWC

Like the rock fragments, also the high sand content (Figure 2) was consistent with the location of the studied soils in proximity to the eruptive source. Several young volcanic soils display coarse textures with low clay content [15,18,77,81–83], and this also occurs under more favorable pedogenetically climatic conditions than those found in the Mediterranean areas [18,21,79]. The detected coarse soil texture, along with rock fragments and permeable lava, assured good drainage and leaching conditions in all studied soil profiles, as expressed by their general low AWC values estimated. Nevertheless, the estimated differences among AWC values also suggested lower leaching efficiency in the finer soils (Soils 1 and 2) than in the coarser ones.

The similarity in grain-size distribution, which, despite the dynamic depositional environment, was observed in most of the studied soil horizons, suggested that the finer particles were more derived from the physical breakdown process than from the direct supply of volcanic ashes, indicating that alteration was at the initial stage. Accordingly, the amount of clay contained in the youngest Soil 6 was minimal because very small particles are only able to accumulate after a prolonged mechanical fragmentation of larger particles. Other young volcanic soils experience physical changes in terms of their primary components, shifting toward finer particles [15,17,31,82] with clay increasing over time [18].

5.3. Chemical Properties

5.3.1. pH, Organic C

Except for Soil 6, pH(H₂O) values did not show major differences among the soil horizons (Figure 3). This was in accordance with the similarity in age and composition of the involved substrata and likely due to the release of cations from the tephra substratum in the first stages of alteration [84,85]. Under these conditions, the organic matter also did not appear to be able to effectively counteract the tephra effect, as suggested by the weak inverse relation between soil pH and organic matter content ($R^2 = 0.167$; $p > 0.05$). Soil 6 exhibited the highest pH(H₂O) values (moderately alkaline), which, strengthened by the lack of organic C, were likely due to the effect of the very young tephra age. The values in question could also be dependent on the marine aerosol that influences the rainwater at Mt. Vesuvius [42] after being intercepted at the high elevation of the soil location, especially in the absence of dense vegetation cover. This effect was supported by the anomalous positive correlation between the elevation and pH of the soil profiles ($R^2 = 0.337$; $p > 0.20$).

The contents of organic C (Figure 3) were almost always within limits detected in soils under Mediterranean climatic conditions, displaying comparable age and vegetation [17,19]. The highest concentration of organic C was found in the A soil horizons, with a strong decrease in the bottom soil portion. At least in the forested soil profiles, this could be partly explained by the fact that the main input of organic matter came from litterfall onto the soil surface [86,87]. In the deep Soils 3 and 4, the organic C decrease was stopped in the buried soil horizons, which showed an increase in the values in question. The weak inverse relation between the elevation and organic C content of the soil profiles ($R^2 = 0.312$; $p > 0.20$) was probably due to the interfingering variety of the vegetation along the slopes. However, some evidence of the effects of exposure and vegetation was found when comparing Soils 4 and 3. In particular, the higher organic C in Soil 4 could be caused by either the eastern orientation or the major supply of C to soil mineral layers from the oak plantation rather than by the pine plantation [88] of Soil 3. At the slope facing north, the absence of organic C in Soil 6 was in accordance with the very sparse herbaceous vegetation.

5.3.2. Oxalate Extractable Al and Fe, Al/Si Ratio and Allophane

Alox and Feox contents (Figure 4) testified to the presence of amorphous mineral components, which are typically found in soils from tephra [89–92]. Most values found in the Vesuvian soil horizons agreed with those characterizing young volcanic soils in Mediterranean climates [14,15,17]. The measured values in question were not influenced by the texture of components, as shown by the lack of correlation with sand (Alox: $R^2 = 0.047$; Feox: $R^2 = 0.005$) and clay (Alox: $R^2 = 0.030$; Feox: $R^2 = 0.146$). Similarly, microclimatic variations along the slopes did not appear to affect the measurements, as suggested by the lack of correlation between Alox and Feox contents of the soil profiles and their respective elevations (Alox: $R^2 = 0.125$; $p > 0.20$; Feox: $R^2 = 0.295$; $p < 0.20$). This was likely due to the different ages of the involved substrata and to the local weathering–promoting circumstances, such as acid rain and gas emissions, which can interfere in Alox and Feox formation.

The Al/Si ratios, which increase with the loss of Si [92], ranged from 0.6 to 1.6 in the studied soils (Table 3). These were similar values to those recorded for other basic and young tephra soils in Mediterranean climate conditions [15,19]. In particular, the analysis of the two soils with the highest Al/Si ratios showed that the ratios in Soil 3 were higher overall than those in Soil 1. Thus, Soil 3 showed a higher degree of glass alteration than Soil 1, despite the similarity of the two soils in their topography and vegetation features. This suggested that differences in other soil features affected the process of Si removal and, thus, the weathering rate. Soil particle size and thickness are important features in this process due to their ability to influence the rate of leaching and removal of weathering products [9]. Accordingly, the coarser and thicker Soil 3, also showing lower AWC values, should display better conditions for leaching and Si removal and, thus, higher Al/Si ratios with respect to Soil 1 (Table 3). This result, in agreement with that related to the analcime/leucite ratios discussed later, suggested that both the dimensions and volume of tephra engaged in soil formation had significant effects on soil properties. The conditions described for Soils 1 and 3 could be related to the factor of “water available for leaching”, which is one of the factors driving pedogenetic pathways in the “energy model” theorized by Runge [93] and reported by Schaetzl and Schwenner [94]. A different pedogenetic context was seen in Soil 6, where the poor degree of glass alteration, indicated by the lowest Al/Si ratios, was attributable to the youngest substratum age.

Among the selected Soils 1, 3, and 6, the estimation of allophane, an alteration product rapidly formed from volcanic rocks [1], in relation to Al/Si ratios, was possible only for Soils 1 and 3, which displayed Al/Si values ranging from 1.0 to 1.6 (Table 3). In such soils, the basic composition of the substrata reported above, the low organic C contents, and pHs > 5.5 were conditions that favored allophane formation [5,8] in an environment with moderate levels of moisture [9,84]. Thus, the detected amounts, no higher than 4.5%, were

substantially in the range of values of other young volcanic soils in the Mediterranean climate [15] but lower than those found in young soils in more humid climates [95].

5.4. Mineralogy

5.4.1. General Remarks

The mineralogical assemblage (Figure 5) found in the analyzed fractions of the selected soils was consistent with the composition of the recent Vesuvian substrata [34]. One abundant component was leucite. This is typically detected in several tephra from Somma-Vesuvius [34,36,52,72,96–98], and the recent products were no exception [35,53,99]. The persistence in clays of the highly weatherable minerals recorded in the analyzed sands supported the concept of physical breakdown as a supplier of finer mineral particles. This is consistent with the short duration of pedogenesis. The same was true for the presence of pyroxenes, which are typically mainly concentrated in coarse fractions [9]. However, the presence of analcime in clay also suggests processes of chemical weathering of primary minerals, as will be discussed later.

The presence of primary weatherable minerals, not only in the deeper soil horizons but also in the upper horizons, as seen in Soil 3, suggested frequent additions of substrata [86], as is often recorded in soils with multiple parent materials.

5.4.2. Analcime

In volcanic soils formed on leucite-rich substrata, analcime is frequently associated with leucite, as seen in pedological investigations in central and southern Italy [100–103]. Analcime is documented as being an igneous primary mineral [104,105]. It is detected in some old Vesuvian rocks [106], but it is absent in the recent formations, except as an alteration product [24,35,53,96,99]. This agrees with the low level of analcime found in the coarser fractions of the studied soils.

Secondary analcime is formed in Vesuvian substrata through hydrothermal activity in alkaline solutions from feldspars, volcanic glass, and leucite [72,73,107–115]. Volcanic glass and leucite serve as better precursors due to their easier weatherability. In particular, the analcime formation from leucite is described as both a dissolution/recrystallization process [116] and an ion-exchange reaction ($\text{KAlSi}_2\text{O}_6 + \text{Na}^+ + \text{H}_2\text{O} = \text{NaAlSi}_2\text{O}_6 \cdot \text{H}_2\text{O} + \text{K}^+$) [113,117,118]. Hydrothermal alteration is also a suitable condition for transformation as, under the high temperatures of the post-depositional phases, this is favored by pH increases via acid gases, which promotes the liberation of cations, as shown for glass weathering [119,120]. This pathway could have constituted a source of analcime in the finer soil fractions studied. Nevertheless, the transformation of leucite via ion-exchange reaction could have also occurred during the pedogenetic phases because the ion exchange has been demonstrated at low field temperatures [113,117,118] and can be favored by a finer size of leucite in clay. Further, Na^+ is commonly present in Vesuvian rocks [34] and supplied by marine aerosol intercepted by the Vesuvian slopes [42]. Ion exchange is supported by the analcime/leucite ratios (Figure 6), which were higher in the clays of Soils 1, 3, and 6 than the respective sands and, on the whole, higher in Soil 1 than in Soil 3. In the latter soil, the combination of coarser particle size and greater thickness could enhance Na removal via leaching. This pathway was similar to that recorded for the glass alteration, which reinforced its significance. In Soil 6, the highest analcime/leucite ratio could be promoted by Na availability derived from the youngest cation-rich substratum and by the impact of the aerosol on Vesuvian surfaces at higher elevations [42].

6. Summary and Conclusions

Three pedological covers were recognized: thin and deep soils on lava flows at different depths and loose detritic soils. Soils showed minimal profile differentiation and were frequently found to display layering, reflecting episodic sediment addition. The major factors implicated in the pedogenesis in the studied recent Vesuvian environment, under

a Mediterranean climate and vegetation, were tephra age and sedimentogenic activity. The young age of substrata accounted for the dominance of the coarse soil particle size, particularly amplified in the proximity of the emission center. Additionally, it contributed to the persistence of the weatherable primary minerals in the finest fractions. The rapid eruptive succession and sediment redistribution caused the accumulation of pyroclastics of variable thicknesses, often forming lithological discontinuities. The quite uniform distribution of primary minerals recorded in the soil particle size fractions accounted for a physical process of parent material disruption, producing low amounts of fine fractions. Chemical weathering evidenced mineral modifications towards the active forms of Al and Fe. Chemical weathering was also evidenced in selected soil profiles by glass alteration through Al/Si ratios, the occurrence of allophane, and the formation of analcime in fine soil fractions. With the exception of some cases, we found a general weakness or lack of relationship between soil properties and physiography. This could be due to conditions interfering with the relief influence, such as repeated rejuvenation, a complex distribution of vegetation, and the past geochemical activity of the studied area. In this scenario, two pedogenetic patterns emerged: the one in which the mineral particle size and the soil thickness influenced the transportation of the weathering products, as in soils on lava, and one in which the substratum age and soil site elevation influenced the low degree of mineral alteration, as in the youngest soil on *Gran Cono Vesuviano*. The results suggested that the high pedogenetic potential, caused by the multiple factors engaged in the young volcanic environment, such as the investigated Somma–Vesuvius area, creates conditions for a recognizable differentiation of the initial pedogenetic pathways. The outcomes provide an opportunity to implement the data collection, to trace the direction of pedogenesis, and to offer insights for studies on other young volcanic sites.

Supplementary Materials: The following supporting information can be downloaded at: <https://www.mdpi.com/article/10.3390/soilsystems8020050/s1>, Figure S1: XRD pattern of >2 mm fraction from A horizon of Soil 1; Figure S2: XRD pattern of >2 mm fraction from Bw horizon of Soil 1; Figure S3: XRD pattern of sand and clay fractions from selected horizons of Soil 3; Figure S4: XRD pattern of sand and clay fractions from horizons of Soil 6.

Author Contributions: Conceptualization, A.E.; methodology, A.E. and C.A.; software, A.E. and C.A.; validation, A.E. and C.A.; formal analysis, A.E. and C.A.; investigation, A.E.; resources, A.E.; data curation, A.E. and C.A.; writing—original draft preparation, A.E.; writing—review and editing, A.E. and C.A.; supervision, A.E. and C.A. All authors have read and agreed to the published version of the manuscript.

Funding: The publication of this research was funded by “Ricerca di Ateneo” of the University of Campania “Luigi Vanvitelli”.

Institutional Review Board Statement: Not applicable.

Informed Consent Statement: Not applicable.

Data Availability Statement: The authors confirm that the data supporting the findings are available within the article and Supplementary Materials.

Acknowledgments: The authors thank the reviewers for their constructive comments.

Conflicts of Interest: The authors declare no conflicts of interest.

References

1. Shoji, S.; Dahlgren, R.; Nanzyo, M. Genesis of volcanic ash soils. In *Volcanic Ash Soils. Genesis, Properties and Utilization*; Shoji, S., Nanzyo, M., Dahlgren, R., Eds.; Developments in Soil Science; Elsevier Science Publisher: Amsterdam, The Netherlands, 1993; Volume 21, pp. 37–74.
2. Ugolini, F.C.; Dahlgren, R.A. Soil development in volcanic ash. *Glob. Environ. Res.* **2002**, *6*, 69–81.
3. Shoji, S.; Dahlgren, R.; Nanzyo, M. Classification of volcanic ash soils. In *Volcanic Ash Soils. Genesis, Properties and Utilization*; Shoji, S., Nanzyo, M., Dahlgren, R., Eds.; Developments in Soil Science; Elsevier Science Publisher: Amsterdam, The Netherlands, 1993; Volume 21, pp. 73–100.

4. Chen, J.; Xiao, Q.; Xu, D.; Li, Z.; Chao, L.; Li, X.; Liu, H.; Wang, P.; Zheng, Y.; Liu, X.; et al. Soil microbial community composition and co-occurrence network responses to mild and severe disturbances in volcanic areas. *Sci. Total Environ.* **2023**, *901*, 165889. [[CrossRef](#)]
5. Óskarsson, B.V.; Riishuus, M.S.; Arnalds, O. Climate-dependent chemical weathering of volcanic soils in Iceland. *Geoderma* **2012**, *189–190*, 635–651. [[CrossRef](#)]
6. van Breemen, V.; Buurman, P. *Soil Formation*, 2nd ed.; Kluwer Academic Publishers: Dordrecht, The Netherlands, 2013.
7. Delfosse, T.; Delmelle, P.; Iserentant, A.; Delveaux, B. Contribution of SO₃ to the acid neutralizing capacity of Andosols exposed to strong volcanogenic acid and SO₂ deposition. *Eur. J. Soil Sci.* **2005**, *56*, 113–125. [[CrossRef](#)]
8. D’Oriano, C.; Bertagnini, A.; Cioni, R.; Pompilio, M. Identifying recycled ash in basaltic eruptions. *Sci. Rep.* **2014**, *4*, 5851. [[CrossRef](#)]
9. Dahlgren, R.; Shoji, S.; Nanzyo, M. Mineralogical characteristics of volcanic ash soils. In *Volcanic Ash Soils. Genesis, Properties and Utilization*; Shoji, S., Nanzyo, M., Dahlgren, R., Eds.; Developments in Soil Science; Elsevier Science Publisher: Amsterdam, The Netherlands, 1993; Volume 21, pp. 101–144.
10. Loughnan, F.C. *Chemical Weathering of the Silicates Minerals*; Elsevier: New York, NY, USA, 1969.
11. Adamo, P.; Violante, P. Weathering of rocks and neogenesis of minerals associated with lichen activity. *Appl. Clay Sci.* **2000**, *16*, 229–256. [[CrossRef](#)]
12. Dahlgren, R.A.; Dragoo, J.P.; Ugolini, F.C. Weathering of Mt. St. Helens tephra under a cryic-udic climate regime. *Soil Sci. Soc. Am. J.* **1997**, *61*, 1519–1525. [[CrossRef](#)]
13. Dahlgren, R.A.; Ugolini, F.C.; Casey, W.H. Field weathering rates of Mt. St. Helens tephra. *Geochim. Cosmochim. Acta* **1999**, *63*, 587–598. [[CrossRef](#)]
14. D’Alessandro, W.; Bellomo, S.; Parello, F. Fluorine adsorption by volcanic soils at Mt. Etna, Italy. *Appl. Geochem.* **2012**, *27*, 1179–1188. [[CrossRef](#)]
15. Egli, M.; Nater, M.; Mirabella, A.; Raimondi, S.; Plötze, M.; Alioth, L. Clay minerals, oxyhydroxide formation, element leaching and humus development in volcanic soils. *Geoderma* **2008**, *143*, 101–114. [[CrossRef](#)]
16. Fiantis, D.; Nelson, M.; Shamshuddin, J.; Goh, T.B.; Van Ranst, E. Leaching experiments in recent tephra deposits from Talang volcano (West Sumatra), Indonesia. *Geoderma* **2010**, *156*, 161–172. [[CrossRef](#)]
17. James, P.; Chester, D.K.; Duncan, A.M. Development and spatial distribution of soils on an active volcano: Mt. Etna, Sicily. *Catena* **2016**, *137*, 277–297. [[CrossRef](#)]
18. Kato, T.; Kamijo, T.; Hatta, T.; Tamura, K.; Higashi, T. Initial soil formation processes of volcanogeneous Regosols (Scoriaceous) from Mijake-jima Island, Japan. *Soil Sci. Plant Nutr.* **2005**, *51*, 291–301. [[CrossRef](#)]
19. Lilienfein, J.; Qualls, R.G.; Uselman, S.M.; Bridgham, S.D. Soil formation and organic matter accretion in a young andesitic chronosequence at Mt. Shasta, California. *Geoderma* **2003**, *116*, 249–264. [[CrossRef](#)]
20. Panico, S.C.; Memoli, V.; Santorufo, L.; Esposito, F.; De Marco, A.; Barile, R.; Giulia, M. Linkage between site features and soil characteristics within a Mediterranean volcanic area. *Front. For. Glob. Chang.* **2021**, *3*, 621231. [[CrossRef](#)]
21. Sasaki, R.; Yoshida, M.; Ohtsu, Y.; Miyahira, M.; Ohta, H.; Watanabe, M.; Suzuki, S. Soil formation of new lahar materials derived from Mt. Pinatubo. *Soil Sci. Plant Nutr.* **2003**, *49*, 575–582. [[CrossRef](#)]
22. Shoji, S.; Takahashi, T. Environmental and Agriculture significance of volcanic ash soils. *Glob. Environ. Res.* **2002**, *6*, 113–135.
23. Arnalds, Ö.; Óskarsson, F.; Buurman, P.; Stoops, G.; García-Rodeja, E. *Soils of Volcanic Regions in Europe*; Springer: Berlin/Heidelberg, Germany, 2007; p. 644.
24. Bottini, O. Indagini pedogenetiche su formazioni vulcaniche. In *Memorie Scientifiche*; Francesco Giannini e Figli: Napoli, Italy, 1971; pp. 251–423. Available online: <https://opac.bncf.firenze.sbn.it/Record/SBL0380463> (accessed on 6 November 2023).
25. Buondonno, C.; Buondonno, C.; Ermice, A. Mineralogia dei suoli sulle vulcanoclastiti del Somma-Vesuvio. In Proceedings of the X Meeting Società Italiana di Chimica Agraria, Roma, Italy, 15–18 September 1992; pp. 115–122.
26. Buondonno, C.; Adamo, P.; Ermice, A.; Leone, A.P.; Testasecca, A. Studio di andisuoli in due diversi ambienti dell’Italia meridionale. *Ann. Fac. Agrar.* **1993**, *36–48*. Available online: <https://www.iris.unina.it/handle/11588/327558> (accessed on 6 November 2023).
27. Ermice, A. A pedological case study of volcanoclastically impacted landscapes: The Vesuvian Avellino air-fall deposits, Southern Italy. *Catena* **2017**, *149*, 241–252. [[CrossRef](#)]
28. Lulli, L. Italian volcanic soils. In *Soils of Volcanic Regions in Europe*; Arnalds, Ö., Óskarsson, H., Bartoli, F., Buurman, P., Stoops, G., García-Rodeja, E., Eds.; Springer Science and Business Media: Berlin/Heidelberg, Germany, 2007; pp. 51–67.
29. Murolo, M.; Pugliano, M.L.; Ermice, A. Landfill and natural soils on the Somma-Vesuvius volcanic complex, Italy: Differences and similarities in soil morphology and properties. *Soil Sci.* **2005**, *170*, 652–668. [[CrossRef](#)]
30. Ruberti, D.; Vigliotti, M.; Marzaioli, M.; Pacifico, A.; Ermice, A. Stratigraphic architecture and anthropic impacts on subsoil to assess the intrinsic potential vulnerability of groundwater: The northeastern Campania Plain case study, southern Italy. *Environ. Earth Sci.* **2016**, *71*, 319–339. [[CrossRef](#)]
31. Vacca, A.; Adamo, P.; Pigna, M.; Violante, P. Genesis of tephra-derived soils from Roccamonfina volcano, South Central Italy. *Soil. Sci. Soc. Am. J.* **2003**, *67*, 198–207.

32. Arnò, V.; Principe, C.; Rosi, M.; Santacroce, R.; Sbrana, A.; Sheridan, M.F. Eruptive History. In *Somma-Vesuvius*; Santacroce, R., Ed.; Quaderni de “La Ricerca Scientifica”, Issue 114; Comitato Nazionale delle Ricerche (CNR): Rome, Italy, 1987; Volume 3, pp. 53–103. Available online: <http://geca.area.ge.cnr.it/files/328066.pdf> (accessed on 6 November 2023).
33. Di Vito, M.A.; Sulpizio, R.; Zanchetta, G.; D’Orazio, M. The late Pleistocene pyroclastic deposits of the Campanian Plain: New insights into the explosive activity of Neapolitan volcanoes. *J. Volcanol. Geotherm. Res.* **2008**, *177*, 19–48. [[CrossRef](#)]
34. Joron, J.; Metrich, N.; Rosi, M.; Santacroce, R.; Sbrana, A. Chemistry and petrography. In *Somma-Vesuvius*; Santacroce, R., Ed.; Quaderni de “La Ricerca Scientifica”, Issue 114; Comitato Nazionale delle Ricerche (CNR): Rome, Italy, 1987; Volume 3, pp. 105–173. Available online: <http://geca.area.ge.cnr.it/files/328066.pdf> (accessed on 6 November 2023).
35. Arrighi, S.; Principe, C.; Rosi, M. Violent strombolian and subplinian eruptions at Vesuvius during post-1631 activity. *Bull. Volcanol.* **2001**, *63*, 26–150. [[CrossRef](#)]
36. Principe, C.; Rosi, M.; Santacroce, R.; Sbrana, A. Explanatory notes to the Geological Map. In *Somma-Vesuvius*; Santacroce, R., Ed.; Quaderni de “La Ricerca Scientifica”, Issue 114; Comitato Nazionale delle Ricerche (CNR): Rome, Italy, 1987; Volume 3, pp. 11–51. Available online: <http://geca.area.ge.cnr.it/files/328066.pdf> (accessed on 6 November 2023).
37. Ricciardi, M.; Mazzoleni, S.; La Valva, V. La flora e la vegetazione del Somma-Vesuvio. In *Elementi di Biodiversità del Parco Nazionale del Vesuvio*; Picariello, O., Ed.; Ente Parco del Vesuvio Napoli: Ottaviano, Italy, 2000; pp. 51–65.
38. Parascandola, A. Notizie Vesuviane. L’attuale fase solfatarica del Vesuvio. *Boll. Soc. Nat. Napoli* **1946**, *LV*, 135–139.
39. Casoria, E. Studio analitico dei prodotti delle ultime eruzioni Vesuviane (1891-94 e 1895-96). *Ann. Sc. Agric. Portici* **1903**, *44*. Available online: https://books.google.com/books/about/Annali_della_Regia_Scuola_superiore_di_a.html?id=_oVWuoNnTvEC (accessed on 6 November 2023).
40. Bottini, O. Fattori pedogenetici particolari della regione vesuviana. Gas e sublimazioni vulcaniche. In *Memorie Scientifiche*; Francesco Giannini e Figli: Napoli, Italy, 1971; pp. 399–405. Available online: <https://opac.bncf.firenze.sbn.it/Record/SBL0380463> (accessed on 6 November 2023).
41. Bottini, O. Le piogge caustiche nella regione vesuviana. In *Memorie Scientifiche*; Francesco Giannini e Figli: Napoli, Italy, 1971; pp. 406–414. Available online: <https://opac.bncf.firenze.sbn.it/Record/SBL0380463> (accessed on 6 November 2023).
42. Madonia, P.; Liotta, M. Chemical composition of precipitation at Mt. Vesuvius and Vulcano Island, Italy: Volcanological and environmental implications. *Environ. Earth Sci.* **2010**, *61*, 159–171. [[CrossRef](#)]
43. Ermice, A.; Pugliano, M.L.; Buondonno, A.; Flaminio, G.; Buondonno, C. Volcanic ejecta as soil forming factor on carbonate relieves of the Partenio Mountain (Campanian Apennines). *Boll. Soc. Geol. Ital.* **1999**, *118*, 505–511.
44. Inoue, Y.; Baasansuren, J.; Watanabe, M.; Kamei, H.; Lowe, D.G. Interpretation of pre-AD 472 Roman soils from physicochemical and mineralogical properties of buried tephric paleosols at Somma Vesuviana ruin, southwest Italy. *Geoderma* **2009**, *152*, 243–251. [[CrossRef](#)]
45. Scarciglia, F.; Zumpano, V.; Sulpizio, R.; Terribile, F.; Pulice, I.; La Russa, M.F. Major factors controlling late Pleistocene to Holocene soil development in the Vesuvius area (southern Italy). *Eur. J. Soil Sci.* **2014**, *65*, 406–419. [[CrossRef](#)]
46. Vogel, S.; Märker, M. Comparison of pre-AD 79 Roman paleosols in two contrasting situations around Pompei (Italy). *Geogr. Fis. Din. Quat.* **2012**, *35*, 99–209.
47. Vogel, S.; Märker, M.; Rellini, I.; Hoelzmann, P.; Wulf, S.; Robinson, M.; Steinhübel, L.; Di Maio, G.; Imperatore, C.; Kastenmeier, P.; et al. From a stratigraphic sequence to a landscape evolution model: Late Pleistocene and Holocene volcanism, soil formation and land use in the shade of Mount Vesuvius (Italy). *Quat. Int.* **2015**, *394*, 155–179. [[CrossRef](#)]
48. Bottini, O.; Ulpiani, S. Sulla pedogenesi nelle regioni vulcaniche italiane. *Ann. Fac. Agrar.* **1945**, *IV*, 1–46.
49. Buondonno, C.; Ermice, A.; Testasecca, A. Aspetti della pedogenesi sulle rocce recenti del Somma-Vesuvio. In Proceedings of the IX Meeting Società Italiana di Chimica Agraria, Torino, Italy, 9–11 September 1991; pp. 161–162.
50. Cecconi, S.; Radaelli, L. Minerali argillosi di terreni provenienti da zone vulcaniche. *Ric. Sci.* **1957**, *5*, 1–4.
51. Scandone, R.; Giacomelli, L.; Fattori Speranza, F. Persistent activity and violent strombolian eruptions at Vesuvius between 1631 and 1944. *J. Volcanol. Geotherm. Res.* **2008**, *170*, 167–180. [[CrossRef](#)]
52. Cioni, R.; D’Orlando, C.; Bertagnini, A. Fingerprinting ash deposits of small scale eruptions by their physical and textural features. *J. Volcanol. Geotherm. Res.* **1999**, *177*, 277–287. [[CrossRef](#)]
53. Rosi, M.; Principe, C.; Vecchi, R. The 1631 Vesuvius eruption. A reconstruction based on historical and stratigraphical data. *J. Volcanol. Geotherm. Res.* **1993**, *58*, 151–182. [[CrossRef](#)]
54. Paolillo, A.; Principe, C.; Bisson, M.; Gianardi, R.; Giordano, D.; La Felice, S. Volcanology of the Southwestern sector of Vesuvius volcano, Italy. *J. Maps* **2016**, *12* (Suppl. S1), 425–440. [[CrossRef](#)]
55. Ventura, G.; Vilardo, G.; Bronzino, G.; Gabriele, R.; Nappi, R.; Terranova, C. Geomorphological map of the Somma-Vesuvius volcanic complex (Italy). *J. Maps* **2005**, *1*, 30–37. [[CrossRef](#)]
56. Paone, A. Geochemical evolution of the Mt. Somma-Vesuvius volcano. *Mineral. Petrol.* **2006**, *87*, 53–80. [[CrossRef](#)]
57. Aiuppa, A.; Federico, C.; Allard, P.; Gurrieri, S.; Valenza, M. Trace metal modeling of groundwater-gas-rock interactions in a volcanic aquifer: Mount Vesuvius, Southern Italy. *Chem. Geol.* **2005**, *216*, 289–311. [[CrossRef](#)]
58. Mazzoleni, S.; Ricciardi, M.; Aprile, G.G. Aspetti pionieri della vegetazione del Vesuvio. *Ann. Bot. Roma* **1989**, *XLVII* (Suppl. S6), 97–107.

59. Orsi, G.; de Vita, S.; Di Vito, M.A.; Isaia, R.; Nava, R.; Heiken, G. Facing volcanic and related hazards in the Neapolitan area. In *Earth Sciences in the Cities: A Reader*; Heiken, G., Fakundiny, R., Sutter, J., Eds.; American Geophysical Union: Washington, DC, USA, 2003; Volume 56, pp. 121–170.
60. Cole, P.D.; Scarpati, C. The 1944 eruption of Vesuvius, Italy: Combining contemporary accounts and field study for a new volcanological reconstruction. *Geol. Mag.* **2010**, *147*, 391–415. [[CrossRef](#)]
61. Rosi, M.; Santacroce, R.; Sbrana, A. *Carta Geologica del Complesso Vulcanico Somma-Vesuvio*. Scala 1:25000. Comitato Nazionale delle Ricerche (CNR). Progetto finalizzato geodinamica. Sottoprogetto 3: Sorveglianza dei vulcani attivi e rischio vulcanico. 1987. Available online: <https://repositories.dst.unipi.it/index.php/carte/item/110-carta-geologica-del-complesso-vulcanico-somma-vesuvio> (accessed on 6 November 2023).
62. Soil Science Division Staff. Examination and description of soil profiles. In *Soil Survey Manual*; Ditzler, C., Scheffe, K., Monger, H.C., Eds.; USDA Handbook 18; Government Printing Office: Washington, DC, USA, 2017; pp. 83–233.
63. Gee, G.W.; Bauder, J.W. Particle-size analysis. In *Methods of Soil Analysis: Part 1, Physical and Mineralogical Methods*, 2nd ed.; Klute, A., Ed.; Agronomy Monograph No 9; American Society of Agronomy and Soil Science Society of America (ASA and SSSA): Madison, WI, USA, 1986; pp. 383–411.
64. Rawls, W.J.; Brakensiek, D.L.; Saxton, K.E. Estimation of soil water properties. *Trans. ASAE* **1982**, *25*, 1316–1320. [[CrossRef](#)]
65. Nelson, D.W.; Sommers, L.E. Total carbon, organic carbon, and organic matter. In *Methods of Soil Analyses*; Page, A.L., Ed.; Part 2; American Society of Agronomy and Soil Science Society of America (ASA and SSSA): Madison, WI, USA, 1982; pp. 539–579.
66. Loepfert, R.H.; Suarez, D.L. Carbonate and gypsum. In *Methods of Soil Analysis. Part 3. Chemical Methods*; Sparks, D.L., Ed.; Soil Science Society of America (SSSA): Madison, WI, USA, 1996; pp. 437–474.
67. Soil Survey Staff. *Keys to Soil Taxonomy*, 13th ed.; USDA-Natural Resources Conservation Service: Washington, DC, USA, 2022; p. 402.
68. Schwertmann, U. The differentiation of iron oxide in soils by a photochemical extraction with ammonium oxalate. *Z. Pflanzenernah. Dung. Bodenkd.* **1964**, *105*, 194–201. [[CrossRef](#)]
69. Blakemore, L.C.; Searle, P.L.; Dealy, B.K. *Methods for Chemical Analyses of Soils*; New Zealand Soil Bureau: Lower Hutt, New Zealand, 1987.
70. Mizota, C.; van Reeuwijk, L.P. *Clay Mineralogy and Chemistry of Soils Formed in Volcanic Material in Diverse Climatic Regions*; International Soil Reference and Information Center: Wageningen, The Netherlands, 1989.
71. Joint Committee on Powder Diffraction Standards. *Selected Powder Diffraction Data for Minerals. Data Book*, 1st ed.; Publ. DBM-1-23; Swarthmore, PA, USA, 1974; Available online: <https://search.worldcat.org/title/Selected-powder-diffraction-data-for-minerals/oclc/819077> (accessed on 6 November 2023).
72. Franco, E.; Petti, C.; Stanzone, D.; Ghiara, M.R.; Marchettiello, A. Studi sugli equilibri chimici e sui minerali di neoformazione nell'interazione H₂O-leucite. *Boll. Soc. Nat. Napoli* **1990**, *98–99*, 25–39.
73. Baldar, N.A.; Whittig, L.D. Occurrence and synthesis of soil zeolites. *Soil Sci. Soc. Am. Proc.* **1968**, *32*, 235–238. [[CrossRef](#)]
74. Nanzyo, M.; Shoji, S.; Dahlgren, R. Physical characteristics of volcanic ash soils. In *Volcanic Ash Soils. Genesis, Properties and Utilization*; Shoji, S., Nanzyo, M., Dahlgren, R., Eds.; Developments in Soil Science; Elsevier Science Publisher: Amsterdam, The Netherlands, 1993; Volume 21, pp. 189–208.
75. Ming, D.W.; Mumpton, F.A. Zeolites in soils. In *Minerals in Soil Environments*, 2nd ed.; Dixon, J.B., Weed, S.B., Eds.; Soil Science Society of America: Madison, WI, USA, 1989; pp. 873–911.
76. Walkers, G.P.L. Grain-size characteristics of pyroclastic deposits. *J. Geol.* **1971**, *79*, 696–714. [[CrossRef](#)]
77. Arnalds, O.; Kimble, J. Andisols of Deserts in Iceland. *Soil Sci. Soc. Am. J.* **2001**, *65*, 1778–1786. [[CrossRef](#)]
78. Arnalds, O.; Hallmark, C.T.; Wilding, L.P. Andisols from four different regions of Iceland. *Soil. Sci. Soc. Am. J.* **1995**, *59*, 161–169. [[CrossRef](#)]
79. Nieuwenhuys, A.; Jongmans, G.; van Breemen, N. Andisol formation in a Holocene beach ridge plain under the humid tropical climate of the Atlantic coast of Costa Rica. *Geoderma* **1993**, *57*, 423–442. [[CrossRef](#)]
80. Schaetzl, R.J.; Anderson, S. *Soils. Genesis and Geomorphology*; Cambridge University Press: Cambridge, UK, 2009.
81. Arnalds, O. Volcanic soils of Iceland. *Catena* **2004**, *56*, 3–20. [[CrossRef](#)]
82. Jahn, R.; Stahr, K. Development of soils and site qualities on basic volcanoclastics with special reference to the semiarid environment of Lanzarote, canary Islands, Spain. *Riv. Mex. Cienc. Geol.* **1996**, *13*, 104–112.
83. Kawai, K. 1978 Amorphous Materials of Andosols (Kuroboku) in Japan. *JARQ* **1978**, *12*, 132–137.
84. Arnalds, O. Andosols. In *Encyclopedia of Soil Science*; Chesworth, W., Ed.; Springer: Dordrecht, The Netherlands, 2008; pp. 39–45.
85. Vilmundardóttir, O.K.; Gísladóttir, G.; Lal, R. Early stage development of selected soil profiles along the proglacial moraines of Skaftafellsjökull glacier, SE-Iceland. *Catena* **2014**, *121*, 142–150. [[CrossRef](#)]
86. Birkeland, P.W. *Soils and Geomorphology*; Oxford University Press, Inc.: New York, NY, USA, 1984; p. 372.
87. Jobbagy, E.G.; Jackson, R.B. The vertical distribution of soil organic carbon and its relation to climate and vegetation. *Ecol. Appl.* **2000**, *10*, 423–436. [[CrossRef](#)]
88. De Marco, A.; Arena, C.; Giordano, M.; Virzo De Santo, A. Impact of the invasive tree black locust on soil properties of Mediterranean stone pine-holm oak forests. *Plant Soil* **2013**, *372*, 473–486. [[CrossRef](#)]
89. Allen, B.L.; Hajek, B.F. Mineral occurrence in soil environments. In *Minerals in Soil Environments*, 2nd ed.; Dixon, J.B., Weed, S.B., Eds.; Soil Science Society of America: Madison, WI, USA, 1989; pp. 199–278.

90. Aomine, S.; Wada, K. Differential weathering of volcanic ash and pumice, resulting in formation of hydrated halloysite. *Am. Mineral.* **1962**, *47*, 1024–1048.
91. Gislason, S.R.; Oelkers, E.H. The mechanism, rates and consequences of basaltic glass dissolution: II. An experimental study of the dissolution rates of basaltic glass as a function of pH and temperature. *Geochim. Cosmochim. Acta* **2003**, *67*, 3817–3832. [[CrossRef](#)]
92. Nanzyo, M.; Dahlgren, R.; Shoji, S. Chemical characteristics of volcanic ash soils. In *Volcanic Ash Soils. Genesis, Properties and Utilization*; Shoji, S., Nanzyo, M., Dahlgren, R., Eds.; Developments in Soil Science; Elsevier Science Publisher: Amsterdam, The Netherlands, 1993; Volume 21, pp. 145–188.
93. Runge, E.C.A. Soil development sequence and energy model. *Soil Sci.* **1973**, *3*, 183–193. [[CrossRef](#)]
94. Schaetzl, R.; Schwenner, C. An application of the Runge energy model of soil development in Michigan's upper Peninsula. *Soil Sci.* **2006**, *171*, 152–166. [[CrossRef](#)]
95. Jongmans, A.G.; Van Oort, F.; Buurman, P.; Jaunet, A.M.; van Doesburg, J.D.J. Morphology, chemistry and mineralogy of isotropic aluminosilicates coatings. *Soil Sci. Soc. Am. J.* **1994**, *58*, 501–507. [[CrossRef](#)]
96. Parascandola, A. L'eruzione Vesuviana del marzo 1944. Rendiconto Della Reale Accademia Delle Scienze Fisiche e Matematiche Della Società Reale di Napoli 1945, Serie 4, XIII, 1942–1945. Available online: <https://opac.bncf.firenze.sbn.it/Record/CFI0866008> (accessed on 6 November 2023).
97. Scherillo, A. Le lave e le scorie dell'eruzione vesuviana del marzo 1944. *Ann. Oss. Vesuv.* **1949**, *V*, 169–183.
98. Scherillo, A. Nuovo contributo allo studio dei prodotti dell'eruzione vesuviana del 1944. *Bull. Volcanol.* **1953**, *13*, 129–144. [[CrossRef](#)]
99. Del Moro, A.; Fulignati, P.; Marianelli, P.; Sbrana, A. Magma contamination by direct wall rock interaction: Constraints from xenoliths from the walls of a carbonate-hosted magma chamber (Vesuvius 1944 eruption). *J. Volcanol. Geotherm. Res.* **2001**, *112*, 15–24. [[CrossRef](#)]
100. Buondonno, C. I minerali argillosi del terreno in provincia di Napoli. *Agrochimica* **1966**, *10*, 157–167.
101. Lulli, L.; Bidini, D.; Lorenzoni, P.; Quantin, P.; Raglione, M. *I suoli caposaldo dell'apparato vulcanico di Vico*, 1st ed.; Istituto Sperimentale Studio e Difesa Suolo-Firenze: Firenze, Italy, 1990.
102. Quantin, P.; Lorenzoni, P. Weathering of leucite to clay minerals in tephrites of the Vico Volcano. *Min. Petrog. Acta* **1992**, *35*, 289–296.
103. Rimmelzwaal, A. Soil Genesis and Quaternary Landscape Development in the Tyrrhenian Coastal Area of South-Central Italy. Ph.D. Thesis, University of Amsterdam, Amsterdam, The Netherlands, 1978. Available online: https://books.google.co.jp/books/about/Soil_Genesis_and_Quaternary_Landscape_De.html?id=xNROAQAIAAJ&redir_esc=y (accessed on 6 November 2023).
104. Hay, R.L. Geologic occurrence of zeolites and some associated minerals. *Pure Appl. Chem.* **1986**, *58*, 1339–1342. [[CrossRef](#)]
105. Luth, R.W.; Bowerman, M. Microtextural and powder-diffraction study of analcime phenocrysts in volcanic rocks of the Crowsnest Formation, Southern Alberta, Canada. *Can. Mineral.* **2004**, *42*, 897–903. [[CrossRef](#)]
106. Parascandola, A. *Mineralogia e Geologia*, 1st ed.; Liguori Editore: Napoli, Italy, 1972; p. 533.
107. Demény, A.; Harangi, S.; Fórizs, I.; Nagy, G. Primary and secondary features of analcimes formed in carbonate-zeolite ocelli of alkaline basalts (Mecsek Mts., Hungary): Textures, chemical, and oxygen isotopes compositions. *Geochem. J.* **1997**, *31*, 37–47. [[CrossRef](#)]
108. Giampaolo, C.; Lombardi, G. Thermal behaviour of analcimes from two different genetic environments. *Eur. J. Mineral.* **1944**, *6*, 285–289. [[CrossRef](#)]
109. Savage, D.; Rochelle, C.; Moore, Y.; Milodowski, A.; Bateman, K.; Bailey, D.; Mihara, M. Analcime reaction at 25–90 °C in hyperalkaline fluids. *Mineral. Mag.* **2001**, *65*, 571–587. [[CrossRef](#)]
110. de' Gennaro, M.; Langella, A.; Cappelletti, P.; Colella, C. Hydrothermal conversion of trachytic glass to zeolite. 3. Monocationic model glasses. *Clays Clay Miner.* **1999**, *47*, 348–357. [[CrossRef](#)]
111. Tucker, M.E. *Sedimentary Petrology: An Introduction to the Origin of Sedimentary Rocks*, 2nd ed.; Blackwell Scientific Publications: Hoboken, NJ, USA, 1991; p. 272.
112. Deer, A.W.; Howie, R.A.; Zussman, J. *Introduzione ai Minerali che Costituiscono le Rocce*; Zanichelli: Bologna, Italy, 1994.
113. Gupta, A.K.; Yagi, K. *Petrology and Genesis of Leucite-Bearing Rocks*; Springer: Berlin/Heidelberg, Germany, 1980.
114. Slaby, E.; Kozłowski, A. Reconstruction of crystallization temperature of artificially grown H-analcime by means of the IR and fluid inclusion studies. *Acta Geol. Pol.* **2002**, *52*, 385–394.
115. Yuan, J.; Yang, J.; Ma, H.; Liu, C.; Zhao, C. Hydrothermal synthesis of analcime and hydroxycancrinite from K-feldspars in Na₂SiO₃ solution: Characterization and reaction mechanism. *RSC Adv.* **2016**, *6*, 54503–54509. [[CrossRef](#)]
116. Putnis, C.V.; Geisler, T.; Schmid-Beurmann, P.; Stephan, T.; Giampaolo, C. An experimental study of the replacement of leucite by analcime. *Am. Mineral.* **2007**, *92*, 19–26. [[CrossRef](#)]
117. Robert, M.; Tessier, D. Incipient weathering: Some new concepts on weathering, clay formation and organization. In *Weathering, Soils and Paleosols*; Martini, I.P., Chesworth, W., Eds.; Elsevier: Amsterdam, The Netherlands, 1992.
118. Robert, M.; Veneau, G. An experimental evaluation of the effects of pH and concentrations of salts on the alteration of leucite at low temperature. *Geoderma* **1974**, *11*, 209–219. [[CrossRef](#)]

119. de' Gennaro, P.; Cappelletti, A.; Langella, A.; Perrotta, A.; Scarpati, C. Genesis of zeolites in Neapolitan Yellow Tuff: Geological, volcanological and mineralogical evidence. *Contrib. Mineral. Petrol.* **2000**, *139*, 17–35. [[CrossRef](#)]
120. Ghiara, M.R.; Petti, G. Chemical alteration of volcanic glasses and related control by secondary minerals: Experimental studies. *Aquat. Geochem.* **1996**, *1*, 329–354. [[CrossRef](#)]

Disclaimer/Publisher's Note: The statements, opinions and data contained in all publications are solely those of the individual author(s) and contributor(s) and not of MDPI and/or the editor(s). MDPI and/or the editor(s) disclaim responsibility for any injury to people or property resulting from any ideas, methods, instructions or products referred to in the content.